Journal of *Marine Science and Engineering*

MDPI

Article

Mitigation of *Vibrio*-Induced Metabolic Perturbations in *Argopecten purpuratus* Scallop Larvae via Probiotic Pretreatment

Katherine Muñoz-Cerro [1], Leonie Venter [2], Tim Young [2], Andrea C. Alfaro [2], Katherina Brokordt [3] and Paulina Schmitt [1,*]

[1] Grupo de Biomarcadores de Holobiontes Marinos Acuícolas (BIHOMA), Laboratorio de Genética e Inmunología Molecular, Instituto de Biología, Pontificia Universidad Católica de Valparaíso, Valparaíso 2340025, Chile; katherine.munoz@pucv.cl

[2] Aquaculture Biotechnology Research Group, School of Science, Auckland University of Technology, Private Bag 92006, Auckland 1142, New Zealand; leonie.venter@aut.ac.nz (L.V.); tim.young@outlook.co.nz (T.Y.); andrea.alfaro@aut.ac.nz (A.C.A.)

[3] Laboratorio de Fisiología y Genética Marina (FIGEMA), Departamento de Acuicultura, Universidad Católica del Norte, Coquimbo 1781421, Chile; kbrokord@ucn.cl

* Correspondence: paulina.schmitt@pucv.cl

Abstract: Background: The decrease in the production of *Argopecten purpuratus* scallops in Chile is linked to extensive larval deaths in hatcheries caused by bacterial pathogens, particularly *Vibrio* genus, threatening sustainability. Traditional antibiotic practices raise concerns, urging research on eco-friendly strategies like bacterial probiotics. This study explores the metabolic responses of scallop larvae to *Vibrio bivalvicida* and evaluates the impact of the *Psychrobacter* sp. R10_7 probiotic on larval metabolism pre- and post-infection. Materials and Methods: Analysis detected 183 metabolite features, revealing significant changes in larval metabolites during *Vibrio* infection. Larvae pretreated with probiotics showed a metabolic profile comparable to non-infected larvae, indicating low impact on larval metabolome, likely due to probiotics antagonistic effect on pathogens. Results: Arachidonic acid, eicosatrienoic acid, docosahexaenoic acid (DHA), eicosapentaenoic acid (EPA), and docosapentaenoic acid (DPA) were significantly higher in non-pretreated/infected larvae compared to both pretreated/infected and non-pretreated/non-infected larvae, potentially supporting the activation of immune response in non-pretreated larvae to *Vibrio* infection. Identification of 76 metabolites provided insights into scallop larvae metabolome, highlighting the enriched metabolic pathways associated with energy provision and immune response. Conclusions: Probiotic pretreatment may mitigate metabolic disruptions in scallop larvae caused by *Vibrio* infection, suggesting a promising strategy for sustainable scallop production.

Keywords: scallop metabolites; bivalve; probiotic bacteria; pathogenic *Vibrio*; aquaculture

Citation: Muñoz-Cerro, K.; Venter, L.; Young, T.; Alfaro, A.C.; Brokordt, K.; Schmitt, P. Mitigation of *Vibrio*-Induced Metabolic Perturbations in *Argopecten purpuratus* Scallop Larvae via Probiotic Pretreatment. *J. Mar. Sci. Eng.* **2024**, *12*, 1138. https://doi.org/10.3390/jmse12071138

Received: 5 June 2024
Revised: 1 July 2024
Accepted: 4 July 2024
Published: 6 July 2024

1. Introduction

The scallop *Argopecten purpuratus* is an important, commercially valuable bivalve mollusk and a significant resource for the local economy in Chile [1,2]. In recent years, scallop production has gradually declined, partly due to episodes of massive larval mortality. These events have resulted in the complete loss of larvae in hatcheries and therefore the supply of seeds for the aquaculture industry [3]. Mortalities are often associated with bacterial pathogens, primarily from the *Vibrio* genus, which affect the early stages of scallop development during the cultivation process, directly impacting the sustainability of the industry [2,4].

Gram-negative and facultatively anaerobic bacteria such as *Vibrio* are common in aquatic environments and, in some cases, are identified as the primary agents causing mass mortalities in bivalve farming [5]. Recently, the presence of *V. bivalvicida* has been identified as one of the main causes of mass mortalities in scallop larvae [4]. Studies have

demonstrated its potential pathogenicity compared to other strains such as *V. anguillarum* and *V. splendidus*, which have been detected during mortality events [4,6–8]. Infection by *V. bivalvicida* begins with the colonization of the larval intestine, where it will subsequently spread to other organs, leading to clinical symptoms associated with vibriosis, including erratic swimming, torn velum, detachment of ciliated cells in the velum, and bacterial swarming, ultimately resulting in larval death [4].

Practices aimed at reducing these mass mortalities in hatcheries primarily involve the treatment of seawater with antibiotics, which can lead to toxicity [2] and bacterial antibiotic resistance [9]. This has encouraged research into scallop immune responses to understand host resistance mechanisms [10–13] and has driven the search for sustainable and environmentally friendly pathogen-control tools [14,15]. Recent studies have examined how the composition of host-associated microbiota plays a crucial role in the animal's health and its resistance to infections [16]. The microbiota perform beneficial functions for the host, such as pathogen tolerance, nutrient production for supporting energy metabolism, and shaping the immune system [17,18]. Hence, several initiatives to isolate and identify host-associated bacteria for use as probiotics have been undertaken as a strategy to control pathogenic infections [18–22].

Beneficial bacteria are recognized as a vital prophylactic strategy in aquaculture when employed as probiotics, offering a sustainable alternative to the controversial use of antibiotics [8]. Probiotic bacteria serve various functions, including the inhibition of pathogen attachment and colonization, as well as the enhancement of the hosts immune system [23]. Recently, bacteria with probiotic properties were characterized and isolated from *Vibrio*-resistant *A. purpuratus* scallop larvae. Among them, the bacteria *Psychrobacter* sp. R10_7 displayed strong antagonistic activity against the pathogen *V. bivalvicida* and enhanced the immune response of scallop larvae [21]. Scallop larvae that received pretreatment with this probiotic candidate exhibited the following outcomes: (i) no mortality within 24 h post-infection, (ii) an earlier induction of host immune pattern recognition receptors, and (iii) no increase in the overall counts of *Vibrio* spp. after infection with the pathogen *V. bivalvicida* [21]. These results demonstrate that scallop larvae resistant to vibriosis harbor unique bacterial species with probiotic characteristics [21]. After obtaining these results, questions arise regarding the aspects of larval physiology modulated by these probiotics to confer resistance. As a first approach, we delve into the analysis of larval metabolism exposed to pathogens and probiotics.

Marine invertebrates, such as scallops are filter-feeding organisms and are therefore constantly exposed to a large number of microorganisms present in the aquatic environment, which can significantly influence their metabolism [24–27]. In bivalve mollusks, there are numerous reports of pathogenic *Vibrio* causing changes in the metabolome. For instance, alterations in metabolites related to physiological processes, such as osmoregulation and restoration of aerobic respiration after anaerobic conditions, have been observed, including a significant decrease in amino acids, sugars, and other compounds essential for dynamic metabolic adjustment and protein renewal to maintain homeostasis [24]. In some cases, such as in the mussel *Perna canaliculus*, elevated levels of metabolites in the glycolysis pathway for energy production were noted, along with reduced activity of metabolites associated with oxidative stress [25]. These changes suggest the activation of antimicrobial activity in infected mussels, as well as a decrease in fatty acid metabolites, commonly used as an energy reserve, and amino acids supporting the immune response.

Some understanding has also been gained regarding the effects of probiotic pretreatment in mollusks and its impacts on the hosts metabolome, as demonstrated in the abalone (*Haliotis iris*) [28]. Pretreatment with multi-strain probiotics (*Exiguobacterium* JHEb1, *Vibrio* JH1, and *Enterococcus* JHLDc) followed by infection with *V. splendidus* resulted in a dysregulation of metabolites associated with the reactive oxygen species (ROS) involved in glutathione biosynthesis, as well as disruptions in the central carbon metabolism processes [29]. Overall, these studies highlight the intricate nature of immune and metabolic responses to infection. However, much is still unknown about the underlying metabolic

mechanisms of probiotic treatment effects in bivalves which limits the optimal development of sustainable disease remediation strategies. Therefore, it is crucial to further explore metabolic host–microbe interactions in other commercially relevant mollusks.

Studying how probiotic bacteria affect the metabolism of marine bivalves and the changes in host metabolites after a bacterial infection is crucial for the reliable use of probiotics in aquaculture disease control. Consequently, in this study, we examined the metabolic profiles of *A. purpuratus* scallop larvae, both pretreated or not with the previously identified probiotic bacteria *Psychrobacter* sp. R10_7 [21], before and after infection with the pathogen *Vibrio bivalvicida* VPAP30. The results obtained enabled us to identify metabolites and characterize the enriched metabolic pathways across various treatments. Moreover, the findings suggest that pretreatment with this bacterial probiotic could potentially shield scallop larvae by mitigating the metabolic perturbations caused by the *Vibrio* infection. These discoveries provide fresh insights into the ways that probiotics affect larval physiology, endorsing their use in aquaculture disease management.

2. Materials and Methods

2.1. Production of Argopecten purpuratus Scallop Larvae of Multiparent Origin

All experiments that included scallop larvae complied with regulations on the protection of animals used for experimental and scientific purposes [30], and the production of scallop larvae was performed as previously described [12]. Scallop larvae were produced in the Central Marine Culture Laboratory of the Universidad Católica del Norte (LCCM-UCN). To obtain scallop larvae (180 ± 0.5 µm in length), mature adults (7.0 ± 0.5 cm in length) of *A. purpuratus* were collected from a culture at Tongoy Bay (Coquimbo, Chile). The animals were maintained for two days in a 1000 L tank with 18 °C filtered seawater (1 µm) and treated with ultraviolet (UV) light. Spawning of broodstock was induced by exposing mature scallops to a high concentration of microalgae (*Isochrysis galbana* clone T-iso + *Chaetoceros calcitrans* + *Pavlova lutheri*, 17×10^6 cells$\times$mL^{-1}).

Adults were separated once spawning commenced to collect the male and female gametes separately to avoid autogamy. Gamete products were mixed at a ratio of 7:10 sperm per oocyte, and the resulting embryos were incubated in 250 L cylindrical tanks with filtered and UV-sterilized aerated seawater at 18 ± 1 °C until they reached the 180 µm size that corresponds to the scallop veliger larval stage. Larvae were fed daily with 20,000 cells × mL^{-1} of microalgal mix (*Isochrysis galbana* clone T-iso + *Chaetoceros calcitrans* + Pavlova lutheri, 17×10^6 cell$\times$mL^{-1}). Feed rations were adjusted to larval density every other day.

2.2. Scallop Larvae Pretreatment with Probiotic Candidate and Vibrio Infection

Scallop larvae (180 ± 0.5 µm in shell length) (n = 500,000) were collected. The health status of a subsample of larvae was checked before the experiments commenced by visual inspection of their swimming activity and intact velum exhibiting intense cilia movement as described by Rojas et al. [4]. Around 25,000 scallop larvae were placed in a series of 1 L aerated flasks (biological replicates), containing filtered seawater (1 µm), that had been treated with UV light. Seawater quality parameters were maintained at a salinity of 34% and temperature of 18 °C for all replicates. The bacterial probiotic *Psychrobacter* sp. R10_7 was added at 1×10^2 cfu$\times$mL^{-1} in sterile seawater (SSW) and incubated at 18 °C for 18 h as described in Muñoz-Cerro et al. [21].

Subsequently, the affecting dose of 30% (AD30) of *V. bivalvicida* VPAP30 (1×10^3 cfu × mL^{-1}) was administered. This dose was previously defined as the bacterial quantity required to observe 30% of affected larvae at 24 h post-infection, meaning positive infection status [21]. The effect of AD30 infection of *V. bivalvicida* on scallop larvae was determined by evaluating clinical signs, such as erratic swimming, velum detachment, and abnormal cilia movement, as described previously [4].

At 18 h post-probiotic pretreatment, the larvae from four biological replicates of non-pretreated/non-infected (NoPT18h) and pretreated/non-infected (PT18h) experimental

conditions were collected. After 24 h of *Vibrio* infection, another four biological replicates from each of the non-pretreated/non-infected (NoPT24h), non-pretreated/infected (NoPTV+24h), and pretreated/infected (PTV+24h) experimental conditions were collected. The larvae from each flask were collected by filtering the seawater through a mesh, immediately concentrating larvae in a tube, and aspirating excess seawater via pipette. Larval samples were freeze-dried, sealed, and stored until further use.

2.3. Sample Preparation for Metabolomic Analysis and Data Processing

Approximately 30 mg of larval sample together with 20 µL of internal standard ([10 mM] L-alanine-2,2,3,3-d4) were re-freeze-dried and extracted using a two-step methanol–water solution. In brief, 500 mL of cold methanol–water solution (50% MeOH–50% H_2O) was added to the dried samples, vortexed for 1 min, and centrifuged for 10 min at 20.8003× *g* at −9 °C, whereafter the supernatants were collected and placed in a new tube. A volume of 500 mL cold methanol–water solution (80%MeOH–20%H_2O) was added to the pellets, followed by vortex and centrifugation (as before). After combining and freezing the supernatants, the samples were dried in a SpeedVac concentrator before derivatization.

Extracted metabolites were derivatized by methyl chloroformate (MCF) alkylation using in-house protocols. The extracts were resuspended in 400 mL [1 M] sodium hydroxide and transferred to salinized borosilicated glass tubes with 334 mL methanol and 68 mL pyridine. While vortexing the samples, a volume of 40 mL MCF reagent was added to the samples and vortexed for 30 s, followed by a second volume of 40 mL MCF reagent for 30 s. Next, 400 mL of chloroform was added and vortexed for 10 s, and next 800 mL [50 mM] sodium bicarbonate was added and vortexed for a further 10 s. The mixture was centrifuged for 5 min at 1.1743× *g* at 6 °C. The upper aqueous layer was discarded, and approximately 30 mg of anhydrous sodium sulphate was added to remove residual water.

The chloroform phase containing the MCF derivatives was transferred to 2 mL amber CG glass vials fitted with inserts. Quality control (QC) samples were included in every extraction batch by preparing a pooled mixture of larvae from subsamples (across all treatments). Additionally, a derivatized sample blank containing the internal standard, an in-house prepared derivatized amino acid mix, and a non-derivatized alkane mix were also injected and analyzed for QC purposes. The MCF derivatives were analyzed with Agilent GC7890B and autosampler coupled to a MSD5977A, with a quadrupole mass selective detector (EI) operated at 70 eV and using a ZB-1701 GC capillary column (30 m × 250 µm internal diameter × 0.25 µm film thickness) and helium as carrier gas (flow of 1 mL/min).

A sample volume of 1 µL was injected under pulsed splitless mode with the injector temperature set at 290 °C. The GC-oven temperature started at 45 °C for 2 min and was increased with a gradient of 9 °C/min to 180 °C; after 5-min, the temperature was increased from 40 °C/min to 220 °C. After a further 5 min, the temperature increased by 40 °C/min to 240 °C and held for 11.5 min. Finally, the temperature was increased by 40 °C/min until it reached 280 °C, where it was held for a further 16 min. The interface temperature was set to 250 °C, and the quadrupole temperature was set to 250 °C. The mass spectrometer was operated in scan mode, starting after 5.6 min, with a mass range of 40–600 amu and a scan time of 0.1 s. Identification of compounds was carried out using mass spectra acquired in scan mode from 40 to 600 amu, with a detection threshold of 80 ion count [27].

2.4. Data Processing

The raw spectra were processed using AMDIS (v2.66) software. Metabolite identifications and peaks integrations were conducted using the Chemstation version B.04.03 (Agilent Technologies, Inc., Santa Clara, CA, USA) and customized R-XCMS based scripts [31] using an in-house mass spectral library of MCF derivatized commercial standards. Compound identifications were based on matches (>70%) to both the MS spectrum of the derivatized metabolite and its respective retention times. Metabolite identifications were assigned a 'level 1' confidence status [32]. Non-identified features were assigned an 'unknown' status. The data matrices of peak intensities were normalized to the peak intensities of the internal

standard and the respective larval sample biomass (Supplementary Table S1). The raw data supporting the findings of this study are in Supplementary Table S1 and openly accessible on Zenodo at https://zenodo.org/records/12190174 (accessed on 20 June 2024).

2.5. Data Analysis

All statistical analyses, including univariate, multivariate, metabolite pathway, and metabolite–metabolite network analyses of the 193 metabolite features, were performed using the web-based tool MetaboAnalyst 6.0 [33]. The data were filtered by interquartile range (IQR), which was employed to identify and remove 5% of near-constant variables throughout the experimental conditions, resulting in a final selection of 183 metabolite features for analysis. One-way analysis of variance (ANOVA) was employed to ascertain the statistical differences in metabolite abundances among the experimental conditions, with a False Discovery Rate (FDR) value < 0.05 considered significant (Supplementary Table S2).

The metabolite response was further analyzed and visualized in a blocked manner via principal component analysis (PCA) [34] and hierarchical clustering (using Euclidean distance measure and ward clustering method). Experimental groups on the PCA scores plots were delineated using 95% confidence ellipses around each group at 18 h and 24 h. Metabolite enrichment pathway analysis was performed using the 76 identified metabolites, comparing the following conditions: NoPT18h vs. PT18h; NoPT24h vs. PTV+24h; NoPT24h vs. NoPTV+24h and NoPTV+24h vs. PTV+24h. This analysis produced a mapping of the annotated metabolites based on their KEGG identification numbers against the *Strongylocentrotus purpuratus* (purple sea urchin) metabolome pathway library.

This resulted in a scatterplot of the metabolome and its corresponding pathways, categorized according to the *p*-values from the enrichment analysis and the pathway impact value from the pathway topology analysis. Metabolite network analysis was performed using Debiased Sparse Partial Correlation (DSPC), together with a functional enrichment analysis, to determine whether the set of metabolites was functionally enriching a metabolic pathway. Color coding was applied to identify relevant metabolic pathways for each set of metabolites [35,36].

3. Results

3.1. Metabolome Profiling of Scallop Larvae Following Probiotic Pretreatment after Vibrio Infection

We established the metabolite profiles of scallop larvae from the following five different treatments across two different time points: non-pretreated larvae (NoPT18h), and larvae pretreated with probiotic (PT18h) at 18 h; and non-pretreated larvae (NoPT24h); larvae non-pretreated and infected with *Vibrio* (NoPTV+24h); and larvae pretreated with probiotic and infected with *Vibrio* (PTV+24h) at 24 h after the pretreatment. In total, we detected a total of 193 metabolite features, comprising 79 identified metabolites and 114 remaining unknown (Supplementary Table S1). A total of 10 metabolites were removed after data filtering, leaving 76 identified metabolites and 107 unknowns for the metabolite profile analysis.

PCA analysis (Figure 1A) and heatmap analysis with hierarchical clustering (Figure 1B) separated the metabolomes of scallop larvae primarily based on the time of sample collection rather than the treatments. Additionally, data from non-pretreated larvae (NoPT18h) and pretreated larvae with the probiotic (PT18h) clustered together and were distinct from the 24 h samples (Figure 1B). The PCA 2D scores plot reveals that PC1 and PC2 explains 36.9% and 23.2% of the total dataset variance, respectively (Figure 1A). In the heatmap, two distinct clusters of metabolites are discerned, with large differences in the relative abundances of many features based on time (Figure 1B). Furthermore, the heatmap showed that non-infected larvae at 18 h, pretreated and not with the probiotic (NoPT18h and PT18h), display a similar metabolite profile that differed from the infected larvae. In addition, pretreated infected larvae (PTV+24h) grouped closer to non-pretreated non-infected

larvae (NoPT24h) when compared to the non-pretreated/infected larvae (NoPTV+24h) (Figure 1B).

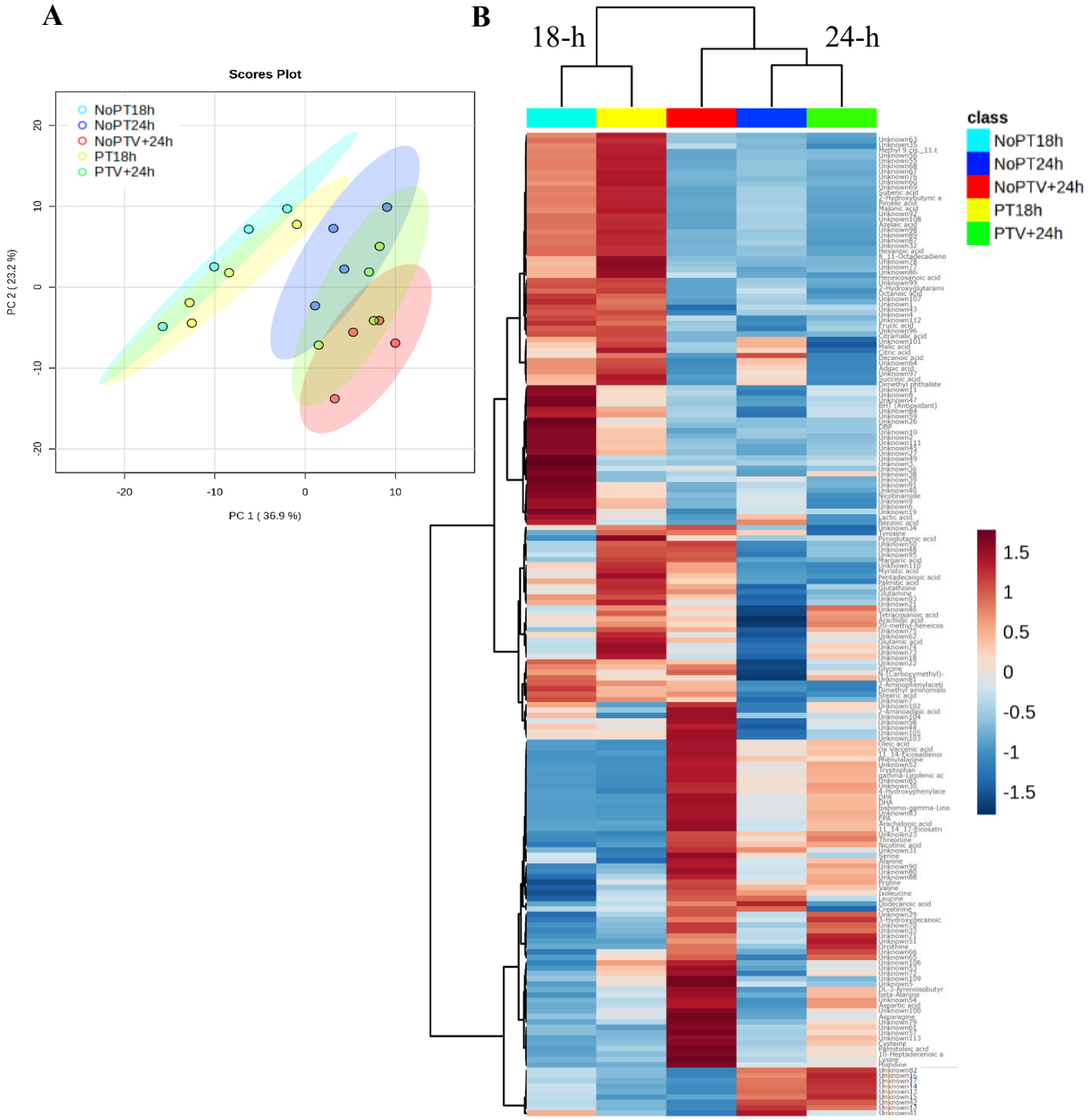

Figure 1. Metabolome profile analysis of *A. purpuratus* larvae from five different treatments. Treatments include the following: no pretreated/no infected 18 h (NoPT18h, light blue), pretreated/no infected 18 h (PT18h, yellow), no pretreated/no infected 24 h (NoPT24h, blue), no pretreated/infected 24 h (NoPTV+24h, red), and pretreated/infected 24 h (PTV+24 h, green). Each treatment comprises four samples of scallop larvae for analysis. (**A**) Principal component analysis (PCA). Samples from the same treatment were highlighted with the use of 95% confidence ellipses around each group. (**B**) Heatmap and hierarchical cluster analysis of 183 metabolite features, highlighting the variation in their mean abundances across different treatments. Values are represented through the color scale from blue (relative low level of abundance) to red (relative high level of abundance).

For a comprehensive examination of how the different treatments affected the levels of each metabolite, metabolite features were analyzed by one-way ANOVA. Significant differences (FDR < 0.05) in the abundances of 35 metabolites (Table 1) and 47 unknowns were detected across treatment groups. Significant differences in metabolite abundances were mainly detected between the 24 h treatments, showing a tendency to increase in larvae non-pretreated and infected with *Vibrio* (NoPTV+24h) and, to a lesser extent, in larvae pretreated with probiotic and infected with *Vibrio* (PTV+24h) compared to the non-pretreated/non-infected control (NoPT24h) (Table 1). On the other hand, only non-significant differences in abundance were found between the non-pretreated (NoPT18h) and pretreated (PT18h) scallop larvae, which exhibit similar trends in the abundance of their metabolites (Table 1). Altogether, these results suggest that the probiotic does not substantially alter the larvae's metabolome at the 18 h pretreatment stage, and that evident metabolite changes in scallop larvae are associated with the *Vibrio* infection.

Table 1. Abundance analysis on the significant 35 metabolites identified in scallop larvae among five different treatments (Supplementary Table S2). The baseline denotes the normalized abundance value of each metabolite across experimental conditions, subsequently compared between the 5 experimental conditions using a two-way ANOVA. Treatments included non-pretreated/non-infected (NoPT18h), pretreated/non-infected (PT18h) larvae at 18 h; and non-pretreated/non-infected (NoPT24h), non-pretreated/infected (NoPTV+24h), and pretreated/infected (PTV+24h) larvae at 24 h. Metabolite abundance is represented by up/down colored arrows indicating significant normalized direction as follows: $\uparrow\uparrow > 2$, $\uparrow > 1$, $\downarrow < -1$, $\downarrow\downarrow < -2$ (FDR < 0.05).

Structural Class	Significant Known Metabolites	FDR	ID	NoPT18h	PT18h	NoPT24h	PTV+24h	NoPTV+24h
Fatty acyls	Arachidonic acid	1.67×10^{-5}	C06425	↓	↓	↓	↑	↑↑
	11,14,17-Eicosatrienoic acid	1.93×10^{-5}	C16522	↓	↓	↓	↑	↑↑
	gamma-Linolenic acid	2.82×10^{-5}	C06426	↓	↓↓	↓	↑	↑↑
	bishomo-gamma-Linolenic acid	5.97×10^{-5}	C03242	↓	↓	↑	↑	↑↑
	Azelaic acid	1.18×10^{-4}	C08261	↑	↑↑	↓	↓	↓
	Suberic acid	1.36×10^{-4}	C08278	↑	↑↑	↓	↓	↓
	11,14-Eicosadienoic	2.49×10^{-4}	C16525	↓	↓	↑	↑	↑↑
	Pimelic acid	2.49×10^{-4}	C02656	↑	↑↑	↓	↓	↓
	cis-Vaccenic acid	1.01×10^{-3}	C08367	↓	↑↑	↑	↑	↓↓
	Oleic acid	1.46×10^{-3}	C00712	↓	↑↑	↑	↑	↓↓
	8,11-Octadecadienoic acid	4.33×10^{-3}	C04056	↑	↓	↓	↓	↑↑
	Adipic acid	4.59×10^{-3}	C06104	↑	↑	↑	↓	↓
	Citramalic acid	6.92×10^{-3}	C00815	↑↑	↑↑	↓	↓	↓
	Hexanoic acid	8.27×10^{-3}	C01585	↑	↑	↓	↓	↓
	Erucic acid	8.46×10^{-3}	C08316	↑	↑	↓	↓	↓
	Heneicosanoic acid	2.16×10^{-2}	0002345	↑	↑	↓	↓	↓
	10-Heptadecenoic acid	2.51×10^{-2}	C16536	↓	↓	↑	↑	↑↑
	Eicosapentaenoic acid (EPA)	1.33×10^{-5}	C06428	↓	↓	↓	↑	↑↑
	Docosahexaenoic acid (DHA)	1.67×10^{-5}	C06429	↓	↓	↓	↑	↑↑
	Docosapentaenoic acid (DPA)	1.67×10^{-5}	C16513	↓	↓	↓	↑	↑↑
	Octanoic acid	3.16×10^{-2}	C06423	↑	↑↑	↓	↓	↓
	Palmitoleic acid	3.80×10^{-2}	C08362	↓	↓	↑	↑	↑↑
Carboxylic acid and derivatives	Threonine	1.33×10^{-5}	C00188	↓↓	↓↓	↑	↑	↑↑
	Malonic acid	8.79×10^{-4}	C00383	↑	↓	↓	↓	↑↑
	Phenylalanine	9.42×10^{-4}	C00079	↓↓	↑↑	↑	↑	↓
	Succinic acid	9.75×10^{-3}	C00042	↑	↑↑	↓	↓	↓
	Cysteine	4.43×10^{-2}	C00097	↓	↓	↓	↑	↑↑
Hydroxy acid and derivatives	2-Hydroxybutyric acid	5.78×10^{-4}	C05984	↑	↑↑	↓	↓	↓
	Lactic acid	1.03×10^{-2}	C00186	↑↑	↑	↑	↓	↓
	3-Hydroxydecanoic acid	1.32×10^{-2}	0010725	↓	↓	↓	↑	↑↑
Benzene and derivatives	Dibutyl phthalate (DBP)	2.67×10^{-3}	C14214	↑↑	↓	↓	↓	↓
	Butylated hydroxytoluene (BHT)	7.61×10^{-3}	C14693	↑↑	↓	↓	↓	↓
Pyridines and derivatives	Nicotinic acid	1.59×10^{-4}	C00253	↓↓	↓	↑	↑	↑↑
Indoles and derivatives	Tryptophan	1.93×10^{-5}	C00078	↓	↓↓	↑	↑	↑↑
Hydroxy dicarboxylic acids	2-Hydroxyglutaramic acid	8.47×10^{-4}	-	↑↑	↑↑	↓	↓	↓

Among the 35 significant metabolites, the abundances of seven were slightly modified at 18 h. Specifically, in pretreated larvae (PT18h), two metabolites showed a slight decrease in abundance (8,11-octadecadienoic acid and malonic acid) compared to NoPT18h control, and two metabolites showed a strong decrease DBP (dibutyl phthalate) and BHT (butylated hydroxytoluene)] compared to NoPT18h control. On the contrary, phenylalanine, cis-vaccenic acid, and oleic acid showed a strong increase compared to NoPT18h control (Table 1).

Following the infection (24 h), a widespread modulation in the abundances of metabolites was observed in the infected larvae (PTV+24h and NoPTV+24h) compared to the control (NoPT24h). Moreover, the intensity of the changes in the abundances was higher in the infected larvae non-pretreated with the probiotic (NoPTV+24h) compared to non-infected larvae, whether pretreated or not (Table 1). Among the 35 significant metabolites, 17 were abundant in non-pretreated/infected larvae (NoPTV+24h). Of these 17 metabolites, 8 showed low abundance in the control NoPT24h, a slight increase in PTV+24h, and an increase in NoPTV+24h; 2 metabolites were poorly represented both in the control (NoPT24h) and in pretreated and infected larvae (PTV+24h) conditions and abundant in No PTV+24h; and 7 metabolites were abundant in the control (NoPT24h) and in pretreated and infected larvae PTV+24h, and strongly abundant in NoPTV+24h.

Interestingly, two metabolites, cis-vaccenic acid and oleic acid, were decreased in the non-pretreated/infected larvae (NoPTV+24h). These metabolites were detected in both low and high concentrations in pretreated larvae under non-infected conditions as well as pretreated and infected conditions, and in pretreated larvae at 18 h (Table 1). Overall, these results suggest that treatment of scallop larvae with the probiotic does not induce major shifts in metabolite abundances at 18 h, and that metabolic perturbations in scallop larvae might be mitigated by probiotic pretreatment.

3.2. Metabolite Structural Classes and Key Enriched Pathways Identified in Scallop Larvae Following Probiotic Pretreatment after Vibrio Infection

Of the 35 known metabolites which were found to be significantly altered among the treatments were classified into the seven structural classes, 22 belong to the fatty acyl class, 5 to carboxylic acid and derivatives, 3 to hydroxy acid and derivatives, 2 to benzene and substituted derivatives, 1 to indoles and derivatives, 1 to hydroxydicarboxylic acids, and 1 to pyridines and derivatives (Table 2). The remaining 41 metabolites showing non-significant differences were categorized into six structural classes as follows: 11 belong to the fatty acyl, 24 to the carboxylic acid and derivatives class, 1 to the hydroxy acid and derivatives, 1 to the benzene and substituted derivatives, 1 to the phenols, and 1 to pyridines and derivatives (Table 2).

Subsequently, metabolic pathway analyses were conducted considering the 76 identified metabolites. They were classified into various metabolic pathways, and pairwise comparisons were performed between treatments (Figure 2, Supplementary Table S3). The results showed that no significantly enriched metabolic pathways were found when comparing the treatments at 18 h, supporting the notion that pretreatment of larvae with the probiotic did not elicit a significant metabolic response at the evaluated time point. However, comparisons between treatments at 24 h revealed several enriched metabolic pathways.

Five enriched metabolic pathways were identified (arachidonic acid metabolism, unsaturated fatty acid biosynthesis, propanoate metabolism, pyrimidine metabolism, and fatty acid biosynthesis) when comparing non-pretreated/infected larvae (NoPTV+24h) with non-pretreated/non-infected larvae (NoPT24h) (Figure 2A). When comparing non-the pretreated/non-infected larvae (NoPT24h) with the pretreated/infected larvae (PTV+24h), four enriched metabolic pathways were identified (pyruvate metabolism, glycolysis and gluconeogenesis, butanoate metabolism, and arachidonic acid metabolism) (Figure 2B).

Table 2. Classification of identified metabolites based on significant and non-significant differences, categorized by their respective structural classes.

Structural Classes	Significant Known Metabolites	Non-Significant Known Metabolites
Fatty Acyls	Arachidonic acid 11,14,17-Eicosatrienoic acid gamma-Linolenic acid bishomo-gamma-Linolenic acid Azelaic acid Suberic acid 11,14-Eicosadienoic Pimelic acid cis-Vaccenic acid Oleic acid 8,11-Octadecadienoic acid Adipic acid Citramalic acid Hexanoic acid Erucic acid Heneicosanoic acid 10-Heptadecenoic acid EPA (Eicosapentaenoic acid) DHA (Docosahexaenoic acid) DPA (Docosapentaenoic acid) Octanoic acid Palmitoleic acid	20-methyl heneicosanoic acid Arachidic acid Decanoic acid Dodecanoic acid Margaric acid Methyl (9Z,11E,13E) Octadecatrienoic acid Myristic acid Palmitic acid Pentadecanoic acid Stearic acid Tetracosanoic acid
Carboxylic acid and derivatives	Threonine Malonic acid Phenylalanine Succinic acid Cysteine	Dimethyl aminomalonic acid N-Carboxymethyl-L-alanine 2-Aminoadipic acid Alanine Asparagine Aspartic acid beta-Alanine Citric acid Creatinine DL-3-Aminoisobutyric acid Glutamic acid Glutamine Glutathione Glycine Histidine Isoleucine Leucine Lysine Ornithine Proline Pyroglutamic acid Serine Tyrosine Valine
Hydroxy acid and derivatives	2-Hydroxybutyric acid Lactic acid 3-Hydroxydecanoic acid	Malic acid
Benzene and substituted derivatives	DBP (Dibutyl phthalate) BHT (Antioxidant)	2-Aminophenylacetic acid Benzoic acid Dimethyl phthalate
Pyridines and derivatives	Nicotinic acid	Nicotinamide
Indoles and derivatives, phenols	Tryptophan	4-Hydroxyphenylacetic acid
Hydroxydicarboxylic acids	2-Hydroxyglutaramic acid	

Finally, four enriched pathways were identified (arachidonic acid metabolism, valine, leucine, and isoleucine biosynthesis, valine, leucine, and isoleucine degradation, and unsaturated fatty acid biosynthesis) in the non-pretreated/infected larvae (NoPTV+24h)

when compared with the pretreated/infected larvae (PTV+24h) (Figure 2C). Altogether, the enrichment analysis revealed a modulation of metabolic pathways associated with energy acquisition in all three comparisons, particularly highlighting arachidonic acid metabolism.

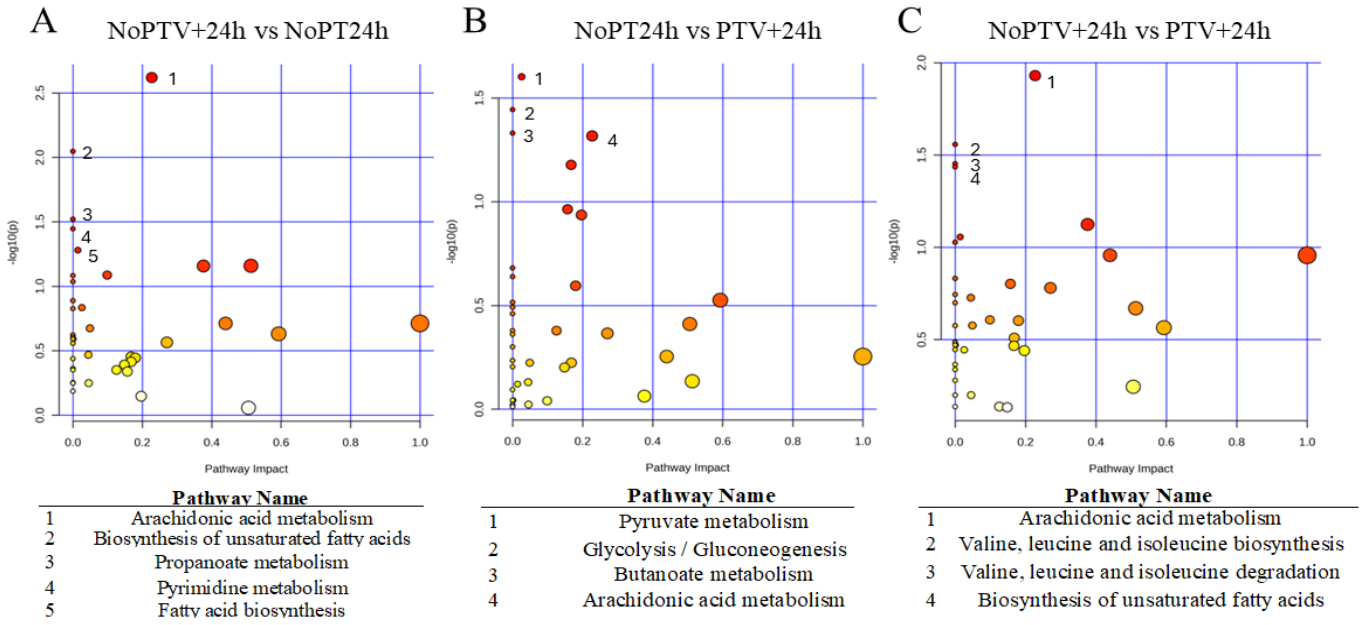

Figure 2. Overview of enriched metabolomic pathways in scallop larvae between different treatments. Enriched metabolic pathways were constructed using the 76 identified metabolites in (**A**) NoPTV+24h vs. NoPT24h, (**B**) NoPT24h vs. PTV+24h and (**C**) NoPTV+24h vs. PTV+24h. Pathways sorted according to enrichment analysis score (Y-axis) and typological analysis (X-axis). The metabolome view shows all enriched pathways as circles. The color (ranging from yellow to red) and size of each circle represent the level of significance and pathway impact value, respectively. Red circles indicate higher statistical significance based on the *p*-value ($p \leq 0.05$; hits ≥ 2).

However, it seems that in response to infection without pretreatment, pathways using fatty acids as precursors are more significantly altered. Conversely, under conditions of pretreatment with the probiotic or in the absence of infection, less alteration in metabolites associated with these pathways is observed, with a pathway more closely linked to energy acquisition through carbohydrates and amino acids.

3.3. Network Analysis Reveals Interconnected Metabolites in Scallop Larvae

We conducted a metabolite network analysis to assess the connections between the 76 identified metabolites (Figure 3). This analysis showed that 39 metabolites were significantly correlated at 18 h, whereas 34 metabolites were significantly correlated at 24 h (Supplementary Table S4). Of these significant metabolites, 17 were shared between the two time points. Significant metabolites were categorized into 10 and 11 metabolic pathways when examined separately at 18 h and 24 h, respectively. In both networks, closely related metabolites share connections, with a notable co- or inverse-regulated direct effect (Figure 3).

Among all the classified metabolites, the majority were found to relate to the unsaturated fatty acid biosynthesis (seven hits) and aminoacyl-transfer ribonucleic acid (tRNA) biosynthesis (seven hits) pathways at both 18 h and 24 h (Figure 3). At 18 h, metabolites associated with fatty acid biosynthesis exhibit a central connection, with some metabolites co-regulated and others inverse-regulated from the center of the network (Figure 3A).

On the other hand, at 24 h, we observed greater indirect connections among the connected metabolites, with the main connectors being those involved in aminoacyl-tRNA biosynthesis and unsaturated fatty acid biosynthesis, all predominantly trending upwards (Figure 3B). Finally, the central position of the energy intermediates such as amino acid,

fatty acid, and derivatives emphasize the importance of energy production in this metabolic network. Moreover, several of the amino acids present are those that normally enter the tricarboxylic acid (TCA) cycle degradation pathway found in the mitochondrial matrix.

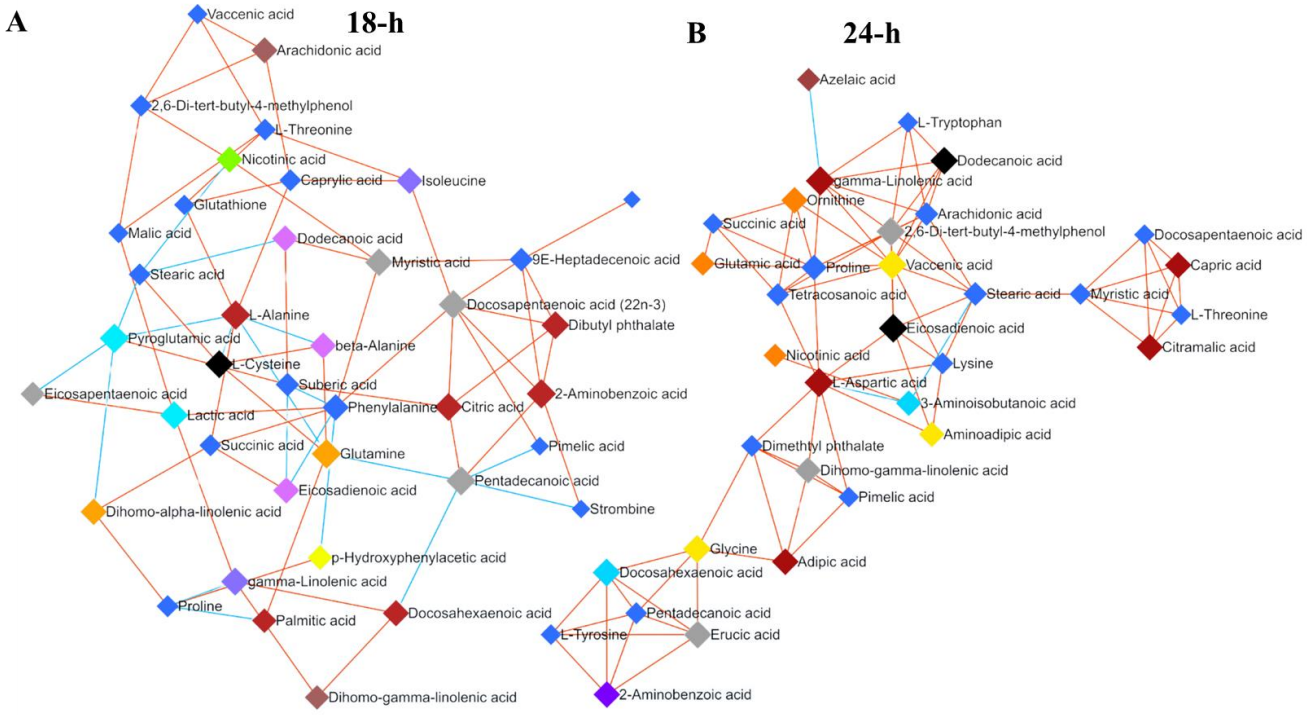

Pathway 18-h	Hits	P.Value	Color
Biosynthesis of unsaturated fatty acids	7	1.26×10^{-6}	
Aminoacyl-tRNA biosynthesis	7	9.66×10^{-6}	
Alanine, aspartate and glutamate metabolism	4	1.12×10^{-3}	
Citrate cycle (TCA cycle)	3	4.41×10^{-3}	
Valine, leucine and isoleucine biosynthesis	2	7.66×10^{-3}	
Fatty acid biosynthesis	4	7.79×10^{-2}	
Glutathione metabolism	3	0.0115	
Glyoxylate and dicarboxylate metabolism	3	0.0167	
Pantothenate and CoA biosynthesis	2	0.0416	
Pyruvate metabolism	2	0.0544	

Pathway 24-h	Hits	P.Value	Color
Aminoacyl-tRNA biosynthesis	8	6.95×10^{-8}	
Biosynthesis of unsaturated fatty acids	5	7.88×10^{-5}	
Arginine biosynthesis	3	7.08×10^{-4}	
Alanine, aspartate and glutamate metabolism	3	5.64×10^{-3}	
Glutathione metabolism	3	5.64×10^{-3}	
Arginine and proline metabolism	3	0.0133	
Butanoate metabolism	2	0.0165	
Nicotinate and nicotinamide metabolism	2	0.0165	
Histidine metabolism	2	0.0187	
Fatty acid biosynthesis	3	0.0237	
Lysine degradation	2	0.0434	

Figure 3. Metabolic networks involved in the enriched metabolic pathways in scallop larvae. The connection between different metabolites is observed at (**A**) 18 h and (**B**) 24 h among significant metabolites from enriched pathways (p-value < 0.05). A color code was employed to discern interactions between metabolites; the color of the line indicates whether the interaction is co-regulated (red line) or inverse-regulated (blue line). Additionally, the color of the square nodes for each metabolite delineates the associated metabolic pathway.

4. Discussion

In this study, we investigated the metabolite profiles of *A. purpuratus* scallop larvae, pretreated or not with a recently discovered bacterial probiotic found in this species [21], and after an infection with the larval pathogen *V. bivalvicida* [4]. The results indicated that (i) the probiotic pretreatment of larvae for 18 h did not significantly alter the host metabolome, (ii) significant changes in metabolites in scallop larvae are mostly associated with the *Vibrio* infection, and (iii) the changes in metabolite abundances of pretreated/infected larvae remained close to those of non-infected larvae after 24 h. These results indicate that metabolic perturbations in scallop larvae could be alleviated through pretreatment with probiotics. Furthermore, the identification of 76 metabolites helped us to gain new insights into the metabolome of scallop larvae, highlighting the enriched metabolic pathways related to the response of scallop larvae to *Vibrio* infection.

The most abundant scallop larval metabolites found in the present study were particularly associated with fatty acids and amino acids, while other metabolites were related to glycolysis and TCA cycle. This suggests that scallop larvae may respond to a pathogenic infection by coordinating a variety of metabolic processes involving the utilization of pro-

teins and fatty acids, providing the energy and resources necessary to support the immune response [37]. Metabolic adaptations occur during a bacterial pathogenic infection in the host, aiming to eliminate the pathogen. These adaptations involve enhancements in specific anabolic pathways, such as amino acid metabolism, along with the modulation of signaling pathways to restrict pathogen invasion and regulate the temporal course of the immune response [38].

The metabolite network revealed that the metabolic pathways used by scallop larvae for energy predominantly involve lipid metabolism. Previous studies have indicated the importance of these types of energy substrates for the scallop larval phase. For instance, in *Placopecten magellanicus*, the accumulation of DHA when fed with an algae-rich diet containing polyunsaturated fatty acids (PUFAs) was suggested to improve the structural and functional integrity of cell membranes for the proper morphological development of larvae [39]. Scallop larvae exhibiting high metamorphic efficiency showed elevated levels of fatty acid reserves, including arachidonic acid, EPA, and DHA. Overall, the results demonstrate that these fatty acids play a crucial role during larval development, serving as an important energy source to meet the energy demands, as described in other mollusk larvae [39,40].

We observed a significant increase in metabolites associated with PUFA biosynthesis under non-pretreated/infected conditions (NoPTV+24h), potentially serving as vital energy support for the immune response to *Vibrio* infections. Here, we showed that the most significant metabolites identified as abundant at 24 h were EPA, DHA, arachidonic acid, and DPA. Apart from their crucial role as an energy source in larvae, they have been described as drivers of immune defense in the presence of pathogens. For instance, increased levels of arachidonic acid and DHA in scallops and mussels have been related to inflammatory responses and modulation of immune function, improving host adaptation to environmental stress [41,42].

Polyunsaturated fatty acids, such as eicosatrienoic acid, DHA, EPA, and DPA, have been related to successful pathogen recognition and phagocytic response associated with the cell membrane in scallops and clams [41,43]. Also, changes in the fatty acid metabolome, along with transcriptional analysis of genes involved in recognition and immune response, have been associated with the modification of the innate immune response at the membrane level in scallops and mussels after pathogenic infections [42,44]. Altogether, this evidence supports the idea that, aside from playing a crucial role during larval development, these fatty acids are essential as an energy source to mount and effective immune response.

In this study, pretreated and infected larvae (PTV+24h) exhibited a metabolic profile that did not significantly differ from that of non-pretreated and non-infected larvae (NoPT24h). This finding suggests that the probiotic's protective effect likely stems from its previously reported antagonist effect against the pathogen [21]. Therefore, the probiotic seems to protect the host by directly combating the pathogen, resulting in a lack of metabolic response in the larvae. However, the probiotic's interaction could significantly influence larval physiology between 18 and 24 h, potentially leading to changes in metabolites. Hence, it is crucial to compare PT24 and NoPT24 to fully understand the impact of probiotic pretreatment on the larval metabolome.

The use of probiotics in aquaculture boosts host immunity and enhances digestive processes, serving as a source of essential amino acids, fatty acids, and vitamins, as observed in shrimp *L. vannamei* and abalone *Haliotis iris* fed with probiotics [28,45]. Another important aspect is that the addition of the probiotic may have contributed to improving the nutritional status of the larvae, reducing the need to induce anabolic pathways to support the energy requirements to face pathogen exposure. For instance, the identified metabolite 3-hydroxydecanoic acid remained unclassified within any metabolic pathway. This is attributed to its characterization as a medium-chain fatty acid produced by bacteria [46]. This metabolite has been shown to exhibit antimitotic activity and is closely linked as a precursor to decanoic acid [47,48]. Furthermore, it is also produced by bacteria from human intestinal microbiota, suggesting that they could contribute to host metabolism [49] and

play a role in cellular damage repair in mammals, making it a therapeutic target in a wide range of diseases [50]. This evidence suggests that the metabolite profile of scallop larvae may be influenced by bacterial metabolites with potential effects on the host physiology and immune response.

The abundance of identified metabolites has revealed the enrichment of specific metabolic pathways during the immune response of scallop larvae. These pathways have been previously associated with energy metabolism from invertebrates such as shrimp, oysters and clams infected with pathogens [51–53]. For instance, the metabolism of fatty acid synthesis, aminoacyl-tRNA synthesis, and arachidonic acid metabolism indicate a potential role in energy demand during an immune response in *P. canaliculus* infected by *V. parahaemolyticus* [25]. Furthermore, the significance of fatty acids as an energy source and membrane component is characteristic of *Vibrio* sp. infections, demonstrating altered lipid metabolism in *Meretrix petechialis* and *P. canaliculus* [27,54].

The metabolic network showed the link between the enriched metabolic pathways, such as fatty acid metabolism, amino acid metabolism, and carbohydrate metabolism. With this approach, the effect of *V. bivalvicida* infection on the metabolic machinery of scallop larvae was highlighted. A metabolic profile similar to the one obtained at 24 h was previously observed in *V. parahaemolyticus*-infected *Meretrix petechialis*, demonstrating that metabolic pathways can directly affect immune response function and promote various associated metabolic routes [54]. In the case of a pathogenic infection, the host's anabolism changes to provide more energy for defense. Therefore, the immune response could be orchestrated along with a metabolic response to optimize the performance of the immune system and enhance host survival [54].

Overall, the identification of metabolite profiles and enriched metabolic pathways in the present study has demonstrated the metabolic modifications in the host response to pathogenic infection, which provides the energy and resources necessary to support the immune response.

5. Conclusions

The identified metabolites indicate that the infection of scallop larvae with *V. bivalvicida* alters larval metabolism, potentially playing a role in energy support and the modulation of the immune response. This is supported by the increased levels of metabolites associated with fatty acid metabolism, aminoacyl-tRNA biosynthesis, arachidonic acid metabolism, amino acid metabolism, and carbohydrate metabolism. Moreover, results suggest that pretreatment with the bacterial probiotic protects scallop larvae by mitigating the metabolic perturbations caused by the *Vibrio* infection. This study represents the first effort to evaluate the impact of probiotic application on the metabolome of scallop larvae.

Supplementary Materials: The following supporting information can be downloaded at: https://www.mdpi.com/article/10.3390/jmse12071138/s1, Table S1: Raw data for detected metabolites in scallop larvae; Table S2: Differences in the abundances of metabolite features in scallop larvae among treatments and metabolite abundance of metabolites normalized; Table S3: Analysis of key metabolic pathways enriched among identified metabolites in scallop larvae between different treatments; Table S4: Network analysis between identified metabolites from 18-h and 24-h treatments.

Author Contributions: K.M.-C., K.B. and P.S. conceived and planned the experiments. K.M.-C. carried out the experiments. T.Y., L.V. and K.M.-C. contributed to sample preparation. A.C.A., K.B., P.S., T.Y., L.V. and K.M.-C. contributed to the interpretation of the results. All authors have read and agreed to the published version of the manuscript.

Funding: This research was funded by the Chilean National Fund for Scientific and Technological Development, FONDECYT #1200129 to P.S. and K.B. K.M. was supported by Beca Doctorado ANID #21201438. Funding for the metabolomics analyses were provided by the Aquaculture Biotechnology Research Group (ABRG) at the Auckland University of Technology (AUT), Auckland, New Zealand.

Institutional Review Board Statement: The animal study protocol was approved by Scientific Ethical Committee of the Universidad Católica del Norte, Chile (Approval number: CEC-UCN N°14).

Informed Consent Statement: Not applicable.

Data Availability Statement: The raw data supporting the conclusions of this article are available on Zenodo at https://zenodo.org/records/12190174.

Acknowledgments: We gratefully acknowledge German Lira and Daniel Aguilera from Laboratorio Central de Cultivos Marinos from UCN for scallop larvae procurement and maintenance. We also thank the members of the Aquaculture Biotechnology Research Group at Auckland University of Technology for their assistance with metabolomics analyses.

Conflicts of Interest: The authors declare no conflicts of interest.

References

1. FAO. *El Estado Mundial de la Pesca y la Acuicultura 2022*; FAO: Rome, Italy, 2022. [CrossRef]
2. Bakit, J.; Álvarez, G.; Díaz, P.A.; Uribe, E.; Sfeir, R.; Villasante, S.; Bas, T.G.; Lira, G.; Pérez, H.; Hurtado, A.; et al. Disentangling Environmental, Economic, and Technological Factors Driving Scallop (*Argopecten purpuratus*) Aquaculture in Chile. *Fishes* **2022**, *7*, 380. [CrossRef]
3. Dubert, J.; Barja, J.L.; Romalde, J.L. New Insights into Pathogenic *Vibrios* Affecting Bivalves in Hatcheries: Present and Future Prospects. *Front. Microbiol.* **2017**, *8*, 762. [CrossRef]
4. Rojas, R.; Miranda, C.D.; Romero, J.; Barja, J.L.; Dubert, J. Isolation and Pathogenic Characterization of *Vibrio bivalvicida* Associated With a Massive Larval Mortality Event in a Commercial Hatchery of Scallop *Argopecten purpuratus* in Chile. *Front. Microbiol.* **2019**, *10*, 855. [CrossRef] [PubMed]
5. Destoumieux-Garzón, D.; Canesi, L.; Oyanedel, D.; Travers, M.; Charrière, G.M.; Pruzzo, C.; Vezzulli, L. *Vibrio*–bivalve interactions in health and disease. *Environ. Microbiol.* **2020**, *22*, 4323–4341. [CrossRef] [PubMed]
6. Rojas, R.; Miranda, C.D.; Opazo, R.; Romero, J. Characterization and pathogenicity of *Vibrio splendidus* strains associated with massive mortalities of commercial hatchery-reared larvae of scallop *Argopecten purpuratus* (Lamarck, 1819). *J. Invertebr. Pathol.* **2015**, *124*, 61–69. [CrossRef] [PubMed]
7. Dubert, J.; Romalde, J.L.; Prado, S.; Barja, J.L. *Vibrio bivalvicida* sp. nov., a novel larval pathogen for bivalve molluscs reared in a hatchery. *Syst. Appl. Microbiol.* **2016**, *39*, 8–13. [CrossRef] [PubMed]
8. Urtubia, R.; Miranda, C.D.; Rodríguez, S.; Dubert, J.; Barja, J.L.; Rojas, R. First Report, Characterization and Pathogenicity of *Vibrio chagasii* Isolated from Diseased Reared Larvae of Chilean Scallop, *Argopecten purpuratus* (Lamarck, 1819). *Pathogens* **2023**, *12*, 183. [CrossRef] [PubMed]
9. Ringø, E. Probiotics in shellfish aquaculture. *Aquac. Fish.* **2020**, *5*, 1–27. [CrossRef]
10. Yue, F.; Shi, X.; Zhou, Z.; Wang, L.; Wang, M.; Yang, J.; Qiu, L.; Song, L. The expression of immune-related genes during the ontogenesis of scallop Chlamys farreri and their response to bacterial challenge. *Fish Shellfish. Immunol.* **2013**, *34*, 855–864. [CrossRef]
11. Rojas, I.; Cárcamo, C.; Stambuk, F.; Mercado, L.; Rojas, R.; Schmitt, P.; Brokordt, K. Expression of immune-related genes during early development of the scallop Argopecten purpuratus after *Vibrio splendidus* challenge. *Aquaculture* **2021**, *533*, 736132. [CrossRef]
12. Rojas, I.; Cárcamo, C.B.; Defranchi, Y.; Jeno, K.; Rengel, J.; Araya, M.; Tarnok, M.E.; Aguilar, L.; Álvarez, G.; Schmitt, P.; et al. A Diet Rich in HUFAs Enhances the Energetic and Immune Response Capacities of Larvae of the Scallop *Argopecten purpuratus*. *Animals* **2023**, *13*, 1416. [CrossRef]
13. Jeria, E.; Oyanedel, D.; Rojas, R.; Farlora, R.; Lira, G.; Mercado, A.; Muñoz, K.; Destoumieux-Garzón, D.; Brokordt, K.; Schmitt, P. Resistance of *Argopecten purpuratus* scallop larvae to *Vibriosis* is associated with the front-loading of immune genes and enhanced antimicrobial response. *Front. Immunol.* **2023**, *14*, 1150280. [CrossRef]
14. Pérez-Sánchez, T.; Mora-Sánchez, B.; Balcázar, J.L. Biological Approaches for Disease Control in Aquaculture: Advantages, Limitations and Challenges. *Trends Microbiol.* **2018**, *26*, 896–903. [CrossRef] [PubMed]
15. Paillard, C.; Gueguen, Y.; Wegner, K.M.; Bass, D.; Pallavicini, A.; Vezzulli, L.; Arzul, I. Recent advances in bivalve-microbiota interactions for disease prevention in aquaculture. *Curr. Opin. Biotechnol.* **2022**, *73*, 225–232. [CrossRef]
16. Lazar, V.; Ditu, L.-M.; Pircalabioru, G.G.; Gheorghe, I.; Curutiu, C.; Holban, A.M.; Picu, A.; Petcu, L.; Chifiriuc, M.C. Aspects of Gut Microbiota and Immune System Interactions in Infectious Diseases, Immunopathology, and Cancer. *Front. Immunol.* **2018**, *9*, 1830. [CrossRef]
17. Li, E.; Xu, C.; Wang, X.; Wang, S.; Zhao, Q.; Zhang, M.; Qin, J.G.; Chen, L. Gut Microbiota and its Modulation for Healthy Farming of Pacific White Shrimp *Litopenaeus vannamei*. *Rev. Fish. Sci. Aquac.* **2018**, *26*, 381–399. [CrossRef]
18. Fallet, M.; Montagnani, C.; Petton, B.; Dantan, L.; de Lorgeril, J.; Comarmond, S.; Chaparro, C.; Toulza, E.; Boitard, S.; Escoubas, J.-M.; et al. Early life microbial exposures shape the Crassostrea gigas immune system for lifelong and intergenerational disease protection. *Microbiome* **2022**, *10*, 85. [CrossRef]
19. Lorgen-Ritchie, M.; Webster, T.U.; McMurtrie, J.; Bass, D.; Tyler, C.R.; Rowley, A.; Martin, S.A.M. Microbiomes in the context of developing sustainable intensified aquaculture. *Front. Microbiol.* **2023**, *14*, 1200997. [CrossRef]

20. Lee, S.-J.; Noh, D.-I.; Lee, Y.-S.; Hasan, T.; Hur, S.W.; Lee, S.; Jeong, S.-M.; Lee, J.M.; Lee, E.-W.; Kim, K.-W.; et al. Effects of host-associated low-temperature probiotics in olive flounder (*Paralichthys olivaceus*) aquaculture. *Sci. Rep.* **2024**, *14*, 2134. [CrossRef]
21. Muñoz-Cerro, K.; González, R.; Mercado, A.; Lira, G.; Rojas, R.; Yáñez, C.; Cuadros, F.; Oyanedel, D.; Brokordt, K.; Schmitt, P. Scallop larvae resistant to a pathogenic *Vibrio* harbor host-associated bacteria with probiotic potential. *Aquaculture* **2024**, *579*, 740217. [CrossRef]
22. Hossain, M.K.; Ishak, S.D.; Iehata, S.; Noordiyana, M.N.; Kader, A.; Abol-Munafi, A.B. Growth performance, fatty acid profile, gut, and muscle histo-morphology of Malaysian mahseer, Tor tambroides post larvae fed short-term host associated probiotics. *Aquac. Fish.* **2024**, *9*, 35–45. [CrossRef]
23. Van Doan, H.; Hoseinifar, S.H.; Ringø, E.; Esteban, M.Á.; Dadar, M.; Dawood, M.A.O.; Faggio, C. Host-Associated Probiotics: A Key Factor in Sustainable Aquaculture. *Rev. Fish. Sci. Aquac.* **2020**, *28*, 16–42. [CrossRef]
24. Frizzo, R.; Bortoletto, E.; Riello, T.; Leanza, L.; Schievano, E.; Venier, P.; Mammi, S. NMR Metabolite profiles of the bivalve mollusc *Mytilus galloprovincialis* before and after immune stimulation with *Vibrio splendidus*. *Front. Mol. Biosci.* **2021**, *8*, 686770. [CrossRef] [PubMed]
25. Ericson, J.A.; Venter, L.; Welford, M.R.; Kumanan, K.; Alfaro, A.C.; Ragg, N.L. Effects of seawater temperature and acute *Vibrio* sp. challenge on the haemolymph immune and metabolic responses of adult mussels (*Perna canaliculus*). *Fish Shellfish. Immunol.* **2022**, *128*, 664–675. [CrossRef] [PubMed]
26. Zhang, Y.; Nie, H.; Yan, X. Metabolomic analysis provides new insights into the heat-hardening response of Manila clam (*Ruditapes philippinarum*) to high temperature stress. *Sci. Total. Environ.* **2023**, *857*, 159430. [CrossRef] [PubMed]
27. Azizan, A.; Carter, J.; Venter, L.; Young, T.; Sharma, S.S.; Chen, T.; Alfaro, A.C. Investigating the effect of bacterial coinfections on juvenile and adult green-lipped mussels (*Perna canaliculus*). *J. World Aquac. Soc.* **2024**, *55*, 386–403. [CrossRef]
28. Grandiosa, R.; Young, T.; Van Nguyen, T.; Mérien, F.; Alfaro, A.C. Immune response in probiotic-fed New Zealand black-footed abalone (*Haliotis iris*) under *Vibrio splendidus* challenge. *Fish Shellfish. Immunol.* **2020**, *104*, 633–639. [CrossRef] [PubMed]
29. Grandiosa, R.; Mérien, F.; Young, T.; Van Nguyen, T.; Gutierrez, N.; Kitundu, E.; Alfaro, A.C. Multi-strain probiotics enhance immune responsiveness and alters metabolic profiles in the New Zealand black-footed abalone (*Haliotis iris*). *Fish Shellfish. Immunol.* **2018**, *82*, 330–338. [CrossRef]
30. Guidelines for the treatment of animals in behavioural research and teaching. *Anim. Behav.* **2020**, *159*, i–xi. [CrossRef]
31. Aggio, R.; Villas−Bôas, S.G.; Ruggiero, K. Metab: An R package for high-throughput analysis of metabolomics data generated by GC-MS. *Bioinformatics* **2011**, *27*, 2316–2318. [CrossRef]
32. Schymanski, E.L.; Jeon, J.; Gulde, R.; Fenner, K.; Ruff, M.; Singer, H.P.; Hollender, J. Identifying Small Molecules via High Resolution Mass Spectrometry: Communicating Confidence. *Environ. Sci. Technol.* **2014**, *48*, 2097–2098. [CrossRef] [PubMed]
33. Pang, Z.; Lu, Y.; Zhou, G.; Hui, F.; Xu, L.; Viau, C.; Spigelman, A.F.; E MacDonald, P.; Wishart, D.S.; Li, S.; et al. MetaboAnalyst 6.0: Towards a unified platform for metabolomics data processing, analysis and interpretation. *Nucleic Acids Res.* **2024**, *52*, W398–W406. [CrossRef] [PubMed]
34. Xu, Y.; Goodacre, R. Multiblock principal component analysis: An efficient tool for analyzing metabolomics data which contain two influential factors. *Metabolomics* **2012**, *8*, 37–51. [CrossRef]
35. Janková, J.; van de Geer, S. Confidence intervals for high-dimensional inverse covariance estimation. *Electron. J. Stat.* **2015**, *9*, 1205–1229. [CrossRef]
36. Basu, S.; Duren, W.; Evans, C.R.; Burant, C.F.; Michailidis, G.; Karnovsky, A. Sparse network modeling and metscape-based visualization methods for the analysis of large-scale metabolomics data. *Bioinformatics* **2017**, *33*, 1545–1553. [CrossRef] [PubMed]
37. Eisenreich, W.; Dandekar, T.; Heesemann, J.; Goebel, W. Carbon metabolism of intracellular bacterial pathogens and possible links to virulence. *Nat. Rev. Microbiol.* **2010**, *8*, 401–412. [CrossRef] [PubMed]
38. Tomé, D. Amino acid metabolism and signalling pathways: Potential targets in the control of infection and immunity. *Eur. J. Clin. Nutr.* **2021**, *75*, 1319–1327. [CrossRef] [PubMed]
39. Pernet, F.; Tremblay, R. Effect of varying levels of dietary essential fatty acid during early ontogeny of the sea scallop *Placopecten magellanicus*. *J. Exp. Mar. Biol. Ecol.* **2005**, *310*, 73–86. [CrossRef]
40. Gagné, R.; Tremblay, R.; Pernet, F.; Miner, P.; Samain, J.-F.; Olivier, F. Lipid requirements of the scallop *Pecten maximus* (L.) during larval and post-larval development in relation to addition of *Rhodomonas salina* in diet. *Aquaculture* **2010**, *309*, 212–221. [CrossRef]
41. Telahigue, K.; Rabeh, I.; Mhadhbi, L.; Nechi, S.; Chelbi, E.; Ben Ali, M.; Hedfi, A.; Al-Harbi, M.S.; Hajji, T. Glyphosate exposure modulates lipid composition, histo-architecture and oxidative stress status and induces neurotoxicity in the smooth scallop *Flexopecten glaber*. *Pestic. Biochem. Physiol.* **2022**, *184*, 105099. [CrossRef]
42. Zhang, Q.; Zhijun, T.; Zheng, G.; Dong, C.; Yang, Y.; Wu, H. The role of Arachidonic acid regulatory network in the metabolism of paralytic shellfish toxins in *Mytilus galloprovincialis*-Based on combined transcriptome and metabolome analysis. *Haiyang Xuebao* **2023**, *45*, 142–152. [CrossRef]
43. Yin, Z.; Nie, H.; Jiang, K.; Yan, X. Molecular Mechanisms Underlying *Vibrio* Tolerance in *Ruditapes philippinarum* Revealed by Comparative Transcriptome Profiling. *Front. Immunol.* **2022**, *13*, 879337. [CrossRef] [PubMed]
44. Zhang, H.; Wang, N.; Zhang, C.; Wang, J.; Ma, H.; Li, S.; Zheng, H. Pathogenesis of black shell disease and its effects on survival and growth in the noble scallop *Chlamys nobilis*. *Aquaculture* **2024**, *578*, 740044. [CrossRef]

45. Alfaro, A.C.; Nguyen, T.V.; Rodríguez, J.A.; Bayot, B.; Domínguez-Borbor, C.; Sonnenholzner, S.; Azizan, A.; Venter, L. Evaluation of immune stimulatory products for whiteleg shrimp (*Penaeus vannamei*) by a metabolomics approach. *Fish Shellfish. Immunol.* **2021**, *120*, 421–428. [CrossRef] [PubMed]
46. Broberg, A.; Jacobsson, K.; Ström, K.; Schnürer, J. Metabolite Profiles of Lactic Acid Bacteria in Grass Silage. *Appl. Environ. Microbiol.* **2007**, *73*, 5547–5552. [CrossRef] [PubMed]
47. Kutschera, A.; Dawid, C.; Gisch, N.; Schmid, C.; Raasch, L.; Gerster, T.; Schäffer, M.; Smakowska-Luzan, E.; Belkhadir, Y.; Vlot, A.C.; et al. Bacterial medium-chain 3-hydroxy fatty acid metabolites trigger immunity in *Arabidopsis* plants. *Science* **2019**, *364*, 178–181. [CrossRef] [PubMed]
48. Divyashree, S.; Shruthi, B.; Vanitha, P.; Sreenivasa, M. Probiotics and their postbiotics for the control of opportunistic fungal pathogens: A review. *Biotechnol. Rep.* **2023**, *38*, e00800. [CrossRef] [PubMed]
49. Qin, F.; Li, J.; Mao, T.; Feng, S.; Li, J.; Lai, M. 2 Hydroxybutyric Acid-Producing Bacteria in Gut Microbiome and *Fusobacterium nucleatum* Regulates 2 Hydroxybutyric Acid Level In Vivo. *Metabolites* **2023**, *13*, 451. [CrossRef] [PubMed]
50. Zheng, N.; Gu, Y.; Hong, Y.; Sheng, L.; Chen, L.; Zhang, F.; Hou, J.; Zhang, W.; Zhang, Z.; Jia, W.; et al. Vancomycin pretreatment attenuates acetaminophen-induced liver injury through 2-hydroxybutyric acid. *J. Pharm. Anal.* **2020**, *10*, 560–570. [CrossRef]
51. Kong, W.; Wu, Z.; Liu, Y.; Yan, C.; Zhang, J.; Sun, Y. RNA-seq analysis revealing the immune response of *Neocaridina denticulata* sinensis gill to *Vibrio parahaemolyticus* infection. *Fish Shellfish. Immunol.* **2022**, *130*, 409–417. [CrossRef]
52. Corporeau, C.; Petton, S.; Vilaça, R.; Delisle, L.; Quéré, C.; Le Roy, V.; Dubreuil, C.; Lacas-Gervais, S.; Guitton, Y.; Artigaud, S.; et al. Harsh intertidal environment enhances metabolism and immunity in oyster (*Crassostrea gigas*) spat. *Mar. Environ. Res.* **2022**, *180*, 105709. [CrossRef] [PubMed]
53. Mao, Y.; Wang, J.; Shi, X.; Liu, Q.; Shao, Y.; Li, C.; Zhao, X. Energy metabolism pathways control the fate of *Sinonovacula constricta* and induction of immune response under *Vibrio parahaemolyticus* challenge. *Aquaculture* **2023**, *569*, 739364. [CrossRef]
54. Yu, J.; Wang, H.; Yue, X.; Liu, B. Dynamic immune and metabolism response of clam *Meretrix petechialis* to *Vibrio* challenge revealed by a time series of transcriptome analysis. *Fish Shellfish. Immunol.* **2019**, *94*, 17–26. [CrossRef] [PubMed]